Calculations of the third-order nonlinear optical responses in push–pull chromophores with a time-dependent density functional theory

Nadya Kobko [1], Artëm Masunov, Sergei Tretiak *

Theoretical Division, Los Alamos National Laboratory, Los Alamos, NM 87545, USA

Abstract

The third-order resonant and static nonlinear optical polarizabilities of the donor–donor and donor–acceptor substituted π conjugated molecules are calculated using the third-order response formalism in combination with time-dependent Hartree–Fock (TD-HF) and density functional theory (TD-DFT) methods. Performance of different levels of theory for excited state structure and nonlinear optical responses has been analyzed. Since the exact computations are fairly expensive, and only a few components of the cubic polarizability (corresponding to the Liouville space paths) are important, numerically efficient approximations are suggested.
© 2004 Elsevier B.V. All rights reserved.

1. Introduction

Optical materials with enhanced nonlinear optical (NLO) responses have important technological implications such as optical switching and wave-guiding [1,2], compact 3D data storage and micro fabrication [3–5], chemical and biological sensing [6,7], optical power limiting [8], up-conversion lasing [9,10], bio-imaging [11,12], etc. Even though perfecting of synthetic techniques and a growing role of quantum mechanical guidance have led to materials with exceptional $\chi^{(2)}$ and $\chi^{(3)}$ hyperpolarizabilities, further progress is still hindered by the cost of both synthetic and characterization methods. In addition, reliable theoretical modeling of real (as oppose to model) molecular systems is yet to be developed.

Computational design of nonlinear optical materials is a fundamentally difficult problem. Careful and comprehensive analysis is necessary for understanding the key electronic phenomena contributing to NLO properties and their related connections with chemical composition. This is a cornerstone for the rational design of new NLO materials. Ab initio techniques coupled with finite field approach are typically used to calculate off-resonant nonlinear optical responses [13]. A more general approach, covering the entire frequency range, is the time dependent perturbation theory. In practice, this is essentially a sum-over-states (SOS) method which involves calculating both ground and excited states wavefunctions and the transition dipole moments between them [13,14]. First-principles calculations of molecular electronic spectra require extensive numerical effort and, therefore, exact treatment becomes impractical even for fairly small molecules. Correct description of excited states involved in NLO responses frequently requires inclusion of the higher order electronic correlations. This makes their computing a much more complicated procedure compared to analogous ground state calculations. For molecules of practical interest it becomes necessary to make various approximations to the underlying many-electron wavefunction. Restricting the size of active space in configuration interaction (CI) to a few orbitals (like in CASSCF), limiting the order of substitutions to singles (CIS) and doubles (CISD), their

---

* Corresponding author. Fax: +1-505-665-3909.

E-mail address: serg@lanl.gov (S. Tretiak).

[1] On leave from the Department of Chemistry, Hunter College and The Graduate School of The City University of New York, 695 Park Avenue, NY 10021, USA.

combination (MRDCI) and/or simplifications in model Hamiltonians (AM1 or INDO/S) are typical examples of such approximations [14,15]. Most of these calculations tend to over-correlate the ground state wavefunction [16,17], and do not guarantee size-consistency [18].

In a contrast with CI-based methods, adiabatic time-dependent density functional theory (TD-DFT) [19,20] in the Kohn–Sham (KS) form has rapidly emerged as an accurate and efficient method for studying the optical response of molecules. Excellent results have been obtained for organic molecules, organometallic compounds, inorganic finite clusters and infinite crystals (e.g., see [21,22]). Recently, TD-DFT extensions for the calculations of molecular nonlinear optical properties were suggested [23–25] and closed expressions for frequency-dependent optical polarizabilities up to the third order in the driving field were derived within adiabatic TD-DFT approximation [25]. TD-DFT was shown to give a better agreement with experiment than both semiempirical and low level ab initio calculations for two-photon absorption (TPA) calculations in large quadrupolar conjugated organic chromophores [26,27] and small molecules [23]. In particular, a benchmark study of TPA and one-photon absorption (OPA) resonant frequencies calculated with TD-DFT (B3LYP/6-31G) against experimental data in a series of 16 substituted molecules found that both TPA and OPA transition energies are predicted with better than 4% accuracy [26]. In a subsequent joint theoretical/experimental study of 6 large molecules we found that TD-DFT (B3LYP/6-31G) can reproduce experimental TPA cross-section with an accuracy better than 50% if experimental linewidths (instead of empirical parameters) were used for calculations [27].

The goal of this Letter is to investigate the methodological aspects of TD-DFT approach for calculations of the third-order NLO properties in extended π-conjugated molecular systems. Since the accuracy of the TD-DFT critically depends on the underlying model of density functional, we study the performance of various exchange–correlation (XC) and hybrid functionals listed in Table 1 for the third-order static and resonant polarizabilities. Several numerical approximations and convergence of the computational results with the number of excited states are investigated as well. We consider two examples: donor–donor substituted case of *para,para'*-bis(dimethylamino)bistyryl and donor–acceptor substituted case of *para*-dimethylamino,*para'*-nitrobistyryl shown in Fig. 1 insets. Substituted bistyryl derivatives were reported to have significant NLO response and experimental NLO data of similar compounds are available [16,17,28]. Details of our computational approach are presented in Section 2. In Section 3 we analyze obtained computational results for different DFT models, regimes, limits, and approximations. Finally, we discuss the trends that emerge and summarize our findings in Section 4.

Table 1
Methods used in this study

Functional	c_x (HF-exchange)	Gradient-correction	LDA component
HF	1	No	No
HF/S	1	No	No
BHandH	0.5	Yes	Yes
MPW1PW91	0.25	Yes	Yes
PBE1PBE	0.25	Yes	Yes
B3LYP	0.2	Yes	Yes
BLYP	0	Yes	Yes
ALDA (Xalpha)	0	No	Yes

The results are obtained using GAUSSIAN 98 [32] implementation of all functionals.
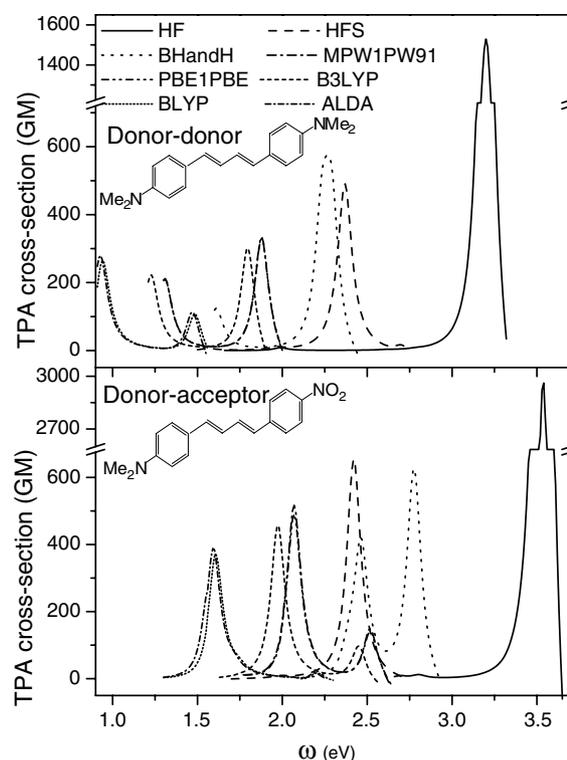
Fig. 1. Calculated TPA spectra of donor–donor (top panel) and donor–acceptor (bottom panel) molecules at different levels of theory (Table 1).

2. Computational methodology

Computation of nonlinear polarizabilities with SOS approach [29] requires ground and excited state energies, state dipoles, and transition dipoles. However, the manifold of contributing states and transition dipole moments between the excited states are not available from the linear response theory [20] (we refer to a detailed discussion in [25]). Alternative expressions for the frequency-dependent polarizabilities have been recently derived specifically for TD-HF and TD-DFT approaches [25,30]. These equations require only quantities that can be obtained from the linear response theory

and the corresponding functional derivatives in the TD-DFT method. The third order polarizability can be calculated using eight term expression symmetrized with respect to ω_1, ω_2, and ω_3 permutations [25]:

$$\gamma_{ijkl}(\omega_1 = \omega, \omega_2 = \omega, \omega_3 = -\omega)$$
$$= \frac{e^4}{6\hbar^3} \sum_{\omega_1,\omega_2,\omega_3}^{\text{perm}} \left(\gamma_{ijkl}^{(\text{I})} + \gamma_{ijkl}^{(\text{II})} + \cdots \gamma_{ijkl}^{(\text{VIII})} \right), \qquad (2.1)$$

where

$$\gamma_{ijkl}^{(\text{I})} = \sum_{\alpha\beta\gamma} \frac{\mu_{-\alpha\beta}^{(j)}\mu_{-\beta\gamma}^{(k)}\mu_{\alpha}^{(i)}\mu_{-\gamma}^{(l)}S_\alpha S_\beta S_\gamma}{(\Omega_\alpha - \omega_1 - \omega_2 - \omega_3)(\Omega_\beta - \omega_2 - \omega_3)(\Omega_\gamma - \omega_3)}, \qquad (2.2)$$

$$\gamma_{ijkl}^{(\text{II})} = \sum_{\alpha\beta\gamma\delta} \frac{-\mu_{-\alpha\beta}^{(j)}V_{-\beta\gamma\delta}\mu_{\alpha}^{(i)}\mu_{-\gamma}^{(k)}\mu_{-\delta}^{(l)}S_\alpha S_\beta S_\gamma S_\delta}{(\Omega_\alpha - \omega_1 - \omega_2 - \omega_3)(\Omega_\beta - \omega_2 - \omega_3)(\Omega_\gamma - \omega_2)(\Omega_\delta - \omega_3)}, \qquad (2.3)$$

$$\gamma_{ijkl}^{(\text{III})} = \sum_{\alpha\beta\gamma} \frac{\mu_{-\alpha\beta\gamma}^{(j)}\mu_{\alpha}^{(i)}\mu_{-\beta}^{(k)}\mu_{-\gamma}^{(l)}S_\alpha S_\beta S_\gamma}{(\Omega_\alpha - \omega_1 - \omega_2 - \omega_3)(\Omega_\beta - \omega_2 - \omega_3)(\Omega_\gamma - \omega_3)}, \qquad (2.4)$$

$$\gamma_{ijkl}^{(\text{IV})} = \sum_{\alpha\beta\gamma\delta} \frac{-2V_{-\alpha\beta\gamma}\mu_{-\gamma\delta}^{(k)}\mu_{\alpha}^{(i)}\mu_{-\beta}^{(j)}\mu_{-\delta}^{(l)}S_\alpha S_\beta S_\gamma S_\delta}{(\Omega_\alpha - \omega_1 - \omega_2 - \omega_3)(\Omega_\beta - \omega_1)(\Omega_\gamma - \omega_2 - \omega_3)(\Omega_\delta - \omega_3)}, \qquad (2.5)$$

$$\gamma_{ijkl}^{(\text{V})} =$$
$$\sum_{\alpha\beta\gamma\delta\eta} \frac{2V_{-\alpha\beta\gamma}V_{-\gamma\delta\eta}\mu_{\alpha}^{(i)}\mu_{-\beta}^{(j)}\mu_{-\delta}^{(k)}\mu_{-\eta}^{(l)}S_\alpha S_\beta S_\gamma S_\delta S_\eta}{(\Omega_\alpha - \omega_1 - \omega_2 - \omega_3)(\Omega_\beta - \omega_1)(\Omega_\gamma - \omega_2 - \omega_3)(\Omega_\delta - \omega_2)(\Omega_\eta - \omega_3)}, \qquad (2.6)$$

$$\gamma_{ijkl}^{(\text{VI})} = \sum_{\alpha\beta\gamma\delta} \frac{-V_{-\alpha\beta\gamma\delta}\mu_{\alpha}^{(i)}\mu_{-\beta}^{(j)}\mu_{-\gamma}^{(k)}\mu_{-\delta}^{(l)}S_\alpha S_\beta S_\gamma S_\delta}{(\Omega_\alpha - \omega_1 - \omega_2 - \omega_3)(\Omega_\beta - \omega_1)(\Omega_\gamma - \omega_2)(\Omega_\delta - \omega_3)}, \qquad (2.7)$$

$$\gamma_{ijkl}^{(\text{VII})} = \sum_{\alpha\beta\gamma} \frac{\mu_{\alpha\beta}^{(i)}\mu_{-\beta\gamma}^{(k)}\mu_{-\alpha}^{(j)}\mu_{-\gamma}^{(l)}S_\alpha S_\beta S_\gamma}{(\Omega_\alpha - \omega_1)(\Omega_\beta - \omega_2 - \omega_3)(\Omega_\gamma - \omega_3)}, \qquad (2.8)$$

$$\gamma_{ijkl}^{(\text{VIII})} = \sum_{\alpha\beta\gamma\delta} \frac{-\mu_{\alpha\beta}^{(i)}V_{-\beta\gamma\delta}\mu_{-\alpha}^{(j)}\mu_{-\gamma}^{(k)}\mu_{-\delta}^{(l)}S_\alpha S_\beta S_\gamma S_\delta}{(\Omega_\alpha - \omega_1)(\Omega_\beta - \omega_2 - \omega_3)(\Omega_\gamma - \omega_2)(\Omega_\delta - \omega_3)}. \qquad (2.9)$$

Here $S_\alpha = \text{sign}(\alpha)$, indices $s = i, j, k, l$ label the spatial directions (x, y, and z), indices $v = \alpha, \beta, \gamma, \delta, \eta = -M, \ldots, M$ run over the excited states, and Ω_v are excitation energies obtained from the linear response theory by diagonalization of the Liouville operator, which eigenvectors (transition densities ξ_v) come in conjugated pairs [20,30]. We assume that Ω_v is positive (negative)

for all $v > 0$ ($v < 0$) according to the convention $\Omega_{-v} = -\Omega_v$. The other variables [25]

$$\mu_\alpha^{(s)} = \text{Tr}(\mu^{(s)}\xi_\alpha), \qquad (2.10)$$

$$\mu_{\alpha\beta}^{(s)} = \sum_{\alpha\beta}^{\text{perm}} \text{Tr}(\mu^{(s)}(I - 2\bar\rho)\xi_\alpha\xi_\beta), \qquad (2.11)$$

$$\mu_{\alpha\beta\gamma}^{(s)} = -\frac{1}{3} \sum_{\alpha\beta\gamma}^{\text{perm}} \text{Tr}(\mu^{(s)}\xi_\alpha\xi_\beta\xi_\gamma), \qquad (2.12)$$

$$V_{\alpha\beta\gamma} = \frac{1}{2} \sum_{\alpha\beta\gamma}^{\text{perm}} \text{Tr}((I - 2\bar\rho)\xi_\alpha\xi_\beta\tilde{V}(\xi_\gamma))$$
$$+ \frac{1}{6} \sum_{\alpha\beta\gamma}^{\text{perm}} \text{Tr}(\xi_\alpha v^{(2)}(\xi_\beta, \xi_\gamma)), \qquad (2.13)$$

$$V_{\alpha\beta\gamma\delta} = \frac{1}{12} \sum_{\alpha\beta\gamma\delta}^{\text{perm}} \text{Tr}((I - 2\bar\rho)\xi_\alpha\xi_\beta\tilde{V}((I - 2\bar\rho)\xi_\gamma\xi_\delta))$$
$$- \frac{1}{12} \sum_{\alpha\beta\gamma\delta}^{\text{perm}} \text{Tr}(\xi_\alpha\xi_\beta\xi_\gamma\tilde{V}(\xi_\delta))$$
$$+ \frac{1}{12} \sum_{\alpha\beta\gamma\delta}^{\text{perm}} \text{Tr}((I - 2\bar\rho)\xi_\alpha\xi_\beta v^{(2)}(\xi_\gamma, \xi_\delta))$$
$$+ \frac{1}{12} \sum_{\alpha\beta\gamma\delta}^{\text{perm}} \text{Tr}(\xi_\alpha v^{(2)}(((I - 2\bar\rho)\xi_\beta\xi_\gamma), \xi_\delta))$$
$$+ \frac{1}{24} \sum_{\alpha\beta\gamma\delta}^{\text{perm}} \text{Tr}(\xi_\alpha v^{(3)}(\xi_\beta, \xi_\gamma, \xi_\delta)) \qquad (2.14)$$

are tensors symmetrized with respect to all permutations of their indices ($\alpha, \beta, \gamma, \delta, \eta$). Here $\mu^{(s)}$ is the dipole matrix for s-spatial direction, $\bar\rho$ is the ground state density matrix, and I is a unit matrix. The Coulomb-exchange–correlation operator $\tilde{V}$ is defined as

$$\tilde{V}_{pq\sigma}(\xi) = \sum_{mn\sigma'} \left((pq\sigma|mn\sigma')\xi_{mn\sigma'} - c_x(pm\sigma|qn\sigma)\xi_{mn\sigma}\delta_{\sigma\sigma'}\right)$$
$$+ \sum_{mn\sigma'} f_{pq\sigma,mn\sigma'}\xi_{mn\sigma'}, \qquad (2.15)$$

where $(pq\sigma|mn\sigma')$ denotes the two-electron integrals (indices p, q, m, n and σ refer to the orbitals spatial and spin indices, respectively). Becke's mixing parameter c_x allows the introduction of Hartree–Fock exchange and the construct of hybrid functionals [31]. $f_{pq\sigma,mn\sigma'}$ is the matrix element of the kernel corresponding to the second functional derivative of an XC functional $E^{xc}[n]$ with respect to the charge density $n(\mathbf{r})$ [19,20]. Finally, the expressions for $v^{(2)}$ and $v^{(3)}$ are quadratic and cubic in ξ, respectively [25], and depend on the third- and fourth-order functional derivatives of $E^{xc}[n]$ [22].

In our implementation of this methodology [26,27] we used the GAUSSIAN 98 package [32] to calculate the linear response in the adiabatic TD-DFT, and to print out the excitation energies Ω_v, transition densities ξ_v, dipole matrices $\mu_v^{(s)}$, and relevant Coulomb-exchange–correlation matrices $\tilde{V}(\xi_v)$ and $\tilde{V}(\frac{1}{2}[[\xi_\beta, \bar{\rho}], \xi_\alpha])$ defined by Eq. (2.15). To calculate the third-order response (Eq. (2.1)) we utilize the Collective Electronic Oscillator (CEO) program [30]. Minor code modifications were required to interface the CEO with TD-DFT data printout, since both TD-HF and TD-DFT methods share the same mathematical description for the excited state electronic structure [25]. In our calculations, terms containing $v^{(2)}$ and $v^{(3)}$ in Eqs. (2.13) and (2.14) have been neglected because the appropriate functional derivatives are not yet available in the GAUSSIAN suite [32] and other similar programs. We believe these quantities may have only a minor impact on polarizability magnitudes [26].

We start our calculations with geometry optimization of both molecules (insets in Fig. 1) at HF/6-31G level with planarity constraint. This method reproduces accurately bond length alternation in such conjugated systems when compared to experiment [26]. This alternation reflects the degree of π-conjugation between the double bonds and constitutes an important parameter characterizing electronic properties in these molecules. TD-DFT calculations were also done with 6-31G basis set. An extension to larger basis sets does not significantly affect the excitation energies and transition dipoles in large conjugated molecules as has been shown in [26]. The solvent effect was studied using polarizable continuum model implemented in GAUSSIAN 98 [33].

We calculated up to 26 singlet electronic states for each molecule using TD-DFT coupled with different functionals listed in Table 1: adiabatic local density approximation (ALDA, also known as Slater exchange), gradient-corrected functional (BLYP), and hybrid functionals (B3LYP, PBE1PBE, MPW1PW91, and BHandH), which contain an increasing portion of exact HF exchange. Calculations using TD-HF approach coupled with ab initio (HF) and semiempirical INDO/S Hamiltonians (HF/S) were conducted as well to explore the limiting case with 100% of HF exchange. The calculations of the static and resonant third-order nonlinear optical polarizabilities were then performed using the procedure described above. The static polarizabilities ($\gamma_0 = Re(\gamma(0,0,0))$) are of interest to a variety of nonlinear applications (i.e. optical switches). We also focus on the resonant response responsible for TPA properties, where the cross-section σ is given as [16,17]:

$$\sigma_{\text{TPA}}(\omega) = \frac{4\pi^2\hbar\omega^2}{5n^2c^2}L^4\text{Im}(\gamma_{xxxx}(\omega,\omega,-\omega)), \quad (2.16)$$

where $\hbar$ is Plank's constant, c is the speed of light, n is the refractive index of the media, L is the local field

factor. Only a dominant component of the polarizability tensor along the molecular axis was included in the average over all orientations. To simulate the finite linewidths in the resonant spectra, an empirical damping factor $\Gamma = 0.1$ eV was introduced in all calculations by adding an imaginary part (iΓ) to the transition frequencies Ω_v in Eqs. (2.2)–(2.9) [16,17,26,27].

3. Results and discussions

Fig. 1 displays the calculated resonant TPA spectra for both molecules obtained at the different levels of theory. The plots clearly show very strong dependence of amplitudes and maxima positions in the computed NLO spectra on the model density functional used. Of all the methods tested, TD-HF results show a significant blue-shift of the largest TPA maximum and highly overestimates its cross-section compared to experiment. On the other hand, ALDA and gradient corrected functionals produce red-shifted spectra. Hybrid functionals span the entire range between the HF and ALDA extremes. Functionals containing 20–25% of the HF exchange result in the most favorable comparison with experiment (see caption to Fig. 2). We also observe two characteristic peaks in the TPA spectra. Their relative magnitudes depend on the functional model. To analyze these resonant spectra in detail, we consider next several relevant quantities.

Fig. 2 illustrates the relationships between the first-order properties of our molecules and the third-order static and resonant polarizabilities. The variation of the transition dipole moments between the ground and the first excited states is shown in the Fig. 2a–a'. For donor–donor molecule, the value of the transition dipoles varies only within 7.25% (from 11.45 D for TD-HF to 12.28 D for TD-PBE1PBE). For donor–acceptor molecule, on the other hand, this value changes considerably (from 7.95 D for TD-BLYP to 11.6 D for TD-HF). This difference reflects electronic delocalization of the excited states: the first excitation in the donor–acceptor compound corresponds to the charge transfer between the two molecular termini, while in the donor–donor molecule it corresponds to the charge transfer from the termini to the central ring [16,17,26]. The HF exchange is known to have a strong effect on the description of the long range interactions, and, therefore, it significantly affects donor–acceptor molecule. Fig. 2b–b' shows the relevant excitation energies. The donor–donor molecule has C_{2h} symmetry, thus its ground ($1A_g$) and the first excited ($1B_u$) states are of the opposite parity. This makes the first excited state with frequency Ω_1 to be inactive in the TPA process. However, the two higher lying states (with frequencies Ω_2 and Ω_n, respectively) show up in the nonlinear spectra (see Fig. 1). In contrast, the donor-acceptor molecule is of C_s symmetry
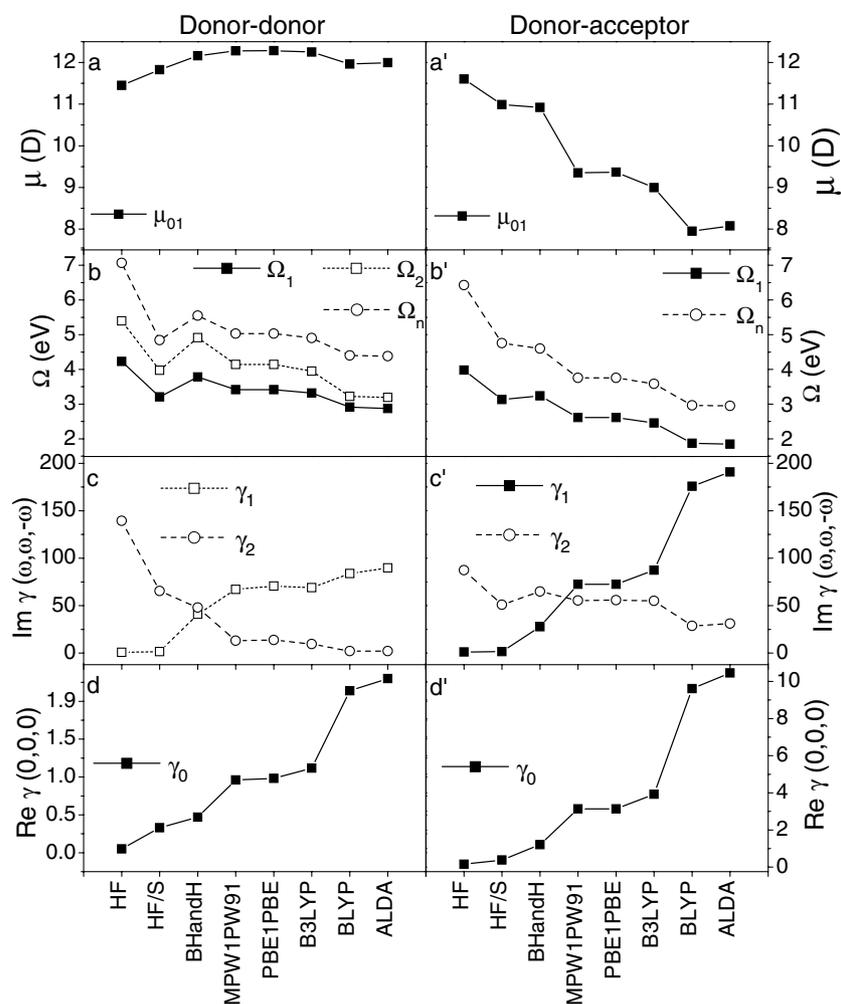
Fig. 2. Transition dipoles between the ground and first excited states (a and a′), transition energies between the ground and excited states contributing to NLO response (b and b′), resonant (c and c′) and static (d and d′) third order polarizabilities (all γ are given in 10^{-33} esu) as a function of DFT model used for calculations. Available experimental data are $\Omega_1 = 3.18$ eV, $\Omega_{TPA} = 3.88$ eV, $\sigma_{TPA} = 260$ GM (donor–donor molecule) [16,17] and $\Omega_1 = 2.72$ eV, $\mu_{01} = 8.9$ D, $\gamma_0 = 1.67 \times 10^{-33}$ esu (donor–acceptor molecule) [28].

and its first excited state manifests itself as the first maximum in Fig. 1. Higher lying state (with frequency Ω_n) is showing in the calculated TPA spectra as well. The excited states of both molecules exhibit large blue shifts with increase of HF exchange fraction in the functional. This fact is due to the nonlocal nature of the HF exchange, which destabilizes the excited states.

Fig. 2c–c′ shows the magnitudes of the third-order polarizabilities at the TPA maxima in Fig. 1 denoted as γ_1 and γ_2. To explain the gradual decrease of the amplitude for the first maximum, and an increase of the amplitude for the second one upon reduction of the amount of the HF exchange, we consider configurational mixing in the resonant excited states of the donor–donor molecule. While the first excited state in this case is mostly HOMO-to-LUMO (highest occupied and lowest unoccupied molecular orbitals) transition, the major contributions to the excited states active in NLO response come from the HOMO-1 to LUMO and HOMO to LUMO+3 configurations. Their out-of-phase

linear combination produces low-amplitude response, while in-phase combination produces high-amplitude response. For a detailed discussion of this effect see [34]. For TD-ALDA, the in-phase combination of these two configurations corresponds to the second excited state and out-of-phase combination to the eighth state. For TD-HF, the relative energies of in-phase and out-of-phase combinations switch. Now they are associated with the sixth and second excited states, respectively. In the case of TD-BHandH, two-photon excited states are represented by almost pure configurations (no configuration mixing takes place), and the amplitudes of the corresponding response maxima are almost equal. Increasing fraction of the HF exchange changes configuration mixing in the lowest two-photon excited state so that one of the components of in-phase combination decreases going from the positive to negative amplitude. As a result, the magnitude of the response decreases.

Unlike the resonant case, the trends in static hyperpolarizability can be interpreted classically. As one can

see in Fig. 2d–d′, the less HF-exchange is present in the functional, the higher values the static polarizabilities acquire. This is in agreement with highly polarizable free electron gas model, inherent to the ALDA functional. We also point out that in all different methods the third-order static polarizablility of the donor-acceptor molecule exceeds that of the donor–donor molecule approximately by a factor of four.

Fig. 3 shows the third-order resonant and static polarizabilities as a function of the number of excited states M used in summations (2.1)–(2.9). In most cases the asymptotic limit is reached with 11 excited states for resonant polarizabilities. However, this is not true for the methods with $c_x \geqslant 0.25$ for both γ_1 and γ_2 maxima (Fig. 3a–a′, b–b′). The absolute values of the third-order polarizability in these cases are very low (see Fig. 2c–c′, d–d′) and, thus, the accuracy of calculations is not sufficient. More states are needed also in the case of the third-order static polarizability (Fig. 3c–c′) where many Liouville space paths contribute to the off-resonant responses.

The solvent effects were studied at B3LYP/6-31G level with polarizable continuum model [33]. We found that nonpolar solvent (such as heptane) changes the resonance response frequency by no more than 0.1 eV (much less for nonpolar donor–donor molecule), and the amplitude at the maximum by about 20% (not shown). More detailed study of the solvent effects on the third-order response properties is currently under way.

To study the effect of the basis set size we calculated both molecules at B3LYP/6-31G* and B3LYP/6-31+G levels. In agreement with results reported previously [26], the basis set size increase changes the polarizability magnitudes by 10 to 20%. The reason for the relatively weak dependence on the basis set lies in the nature of the molecules studied. The third-order response properties are dominated by a delocalized π-electron system, and atomic polarization becomes relatively unimportant. Consequently, addition of the polarization and diffuse functions to the basis set does not change the results substantially.

Finally, Fig. 4 displays the contributions from the different components into the total third-order polarizability for different methods. We observe that the general trends for both molecules are very similar for resonant and static polarizabilities (with the exception of the TD-HF method). In most cases the major contribution comes from $\gamma^{(I)}$ and $\gamma^{(VII)}$ terms. In fact, $\gamma^{(I)}$ and $\gamma^{(VII)}$ depend only on the dipole couplings (Eqs. (2.10) and (2.11)) and are the only terms that give significant contribution into the resonant polarizabilities if HF-exchange is not present in the functional. $\gamma^{(III)}$ always gives negative contribution to the third-order static polarizability. This term contains dipole coupling between three excited states (Eq. (2.12)). None of $\gamma^{(I)}$, $\gamma^{(VII)}$ and $\gamma^{(III)}$ terms contains Coulomb operators. For the resonant polarizability, the second major contribution comes from $\gamma^{(II)}$ and $\gamma^{(VIII)}$ terms, but these contributions
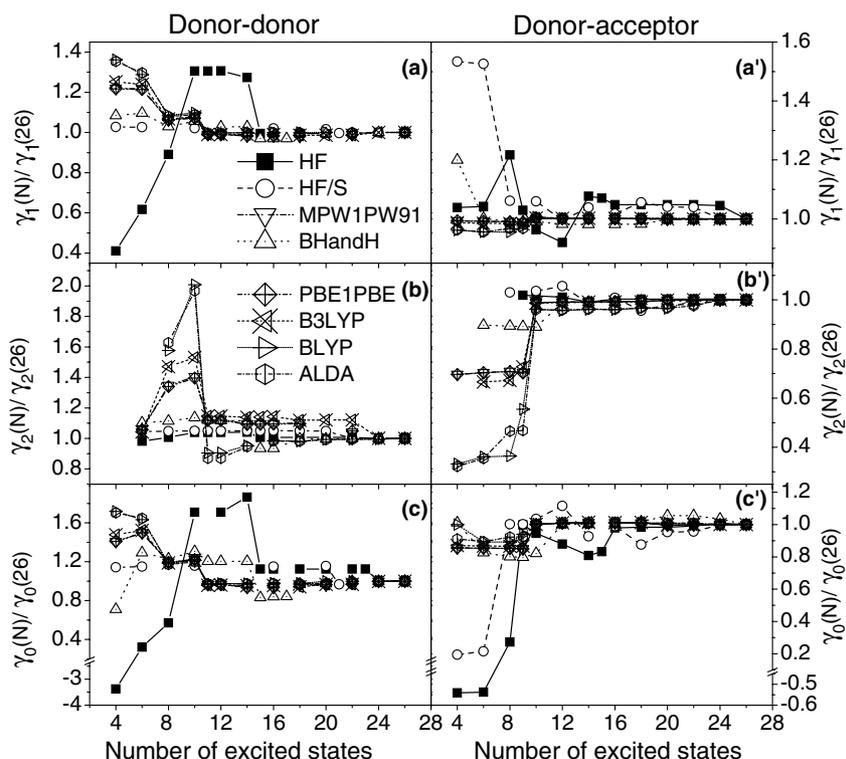
Fig. 3. Variation of magnitudes of resonant polarizabilities at the first (a and a′) and second (b and b′) TPA maxima, and static polarizability (c and c′) with the number of excited states used for calculations.
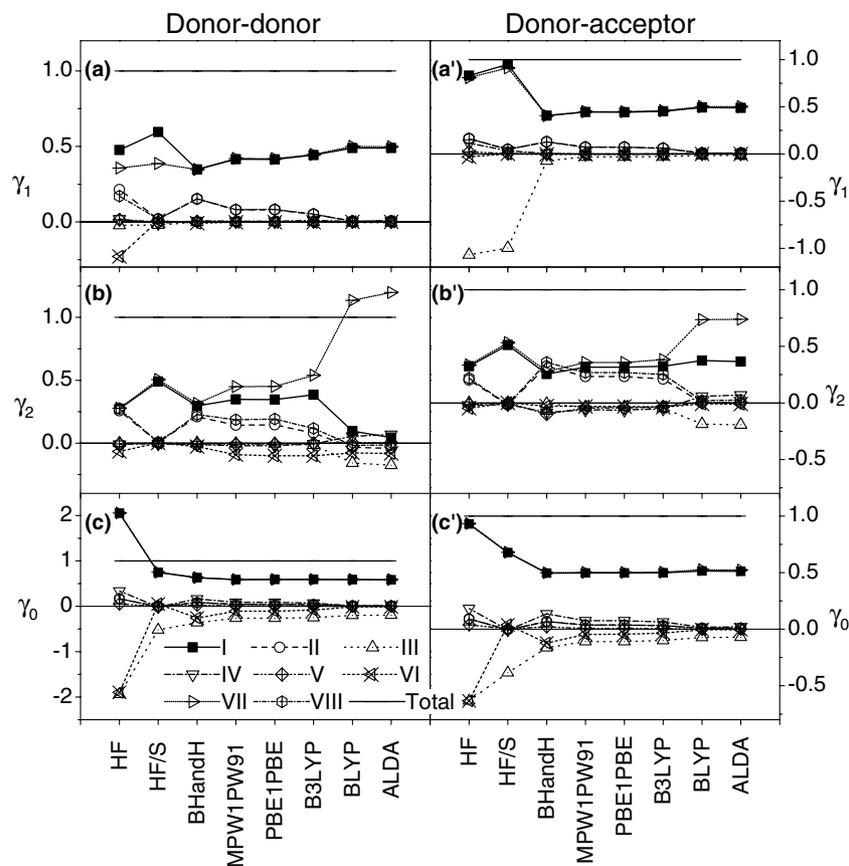
Fig. 4. Relative contributions from different terms in expansion (2.1) to resonant (a, a′ and b, b′) and static (c and c′) NLO responses as a function of DFT model.

amount for less than 8.3% each for the functionals with $c_x \leqslant 0.25$ in the case of the first maximum. However, these terms contribute significantly to TD-BHandH and TD-HF results. Both $\gamma^{(II)}$ and $\gamma^{(VIII)}$ terms contain Coulomb operators coupling three states (Eq. (2.13)) and dipole couplings (Eq. (2.11)). The next (usually negative) contribution comes from $\gamma^{(VI)}$. This term is very small in case of resonant polarizability (except for TD-HF method at the first maximum). For static polarizability, $\gamma^{(VI)}$ term has considerable contribution only in the case of TD-BHandH and pure TD-HF methods. This term (Eq. (2.14)) depends on the Coulomb operator which couples four excited states and, therefore, $\gamma^{(VI)}$ contains most of the computational expense for the third order polarizability. Thus several approximations can be readily applied to significantly reduce the numerical cost of the third-order polarizability calculations depending on the level of accuracy required.

4. Conclusion

Enhanced NLO properties in functional organic and inorganic materials result from the long range electronic 'communication' (coherence and charge transport). The optical response of a large π-conjugated molecular system is not the sum of separate responses of its small components, rather, the response is a nonlinear function of the system size ('collective' effect). Conducting polymers and donor/acceptor substituted conjugated organic chromophores are typical examples of molecules where large optical polarizabilities are attributed to the delocalized nature of their electronic excitations [13,14]. Consequently, full quantum chemical treatment is required for quantitative predictions and, often, qualitative analysis of the underlying phenomena. The TD-DFT approach shows great promises for computing molecular hyperpolarizabilities in such systems. This method is free from many drawbacks inherent to high level correlated methods and provides an excellent accuracy for the entire molecular electronic spectrum and the NLO responses [23,26,27].

A critical component of TD-DFT is a choice of an appropriate functional. We show that TD-ALDA and gradient corrected functionals tend to over-delocalize π-electron system, which frequently leads to the red shifts in the calculated spectra. In contrast, over-localization in the TD-HF method results in the blue shifts of NLO transition energies, increasingly large number of participating excited states, and significant role of Coulomb-related terms in the expansion (2.1). Hybrid

DFT provides balanced treatment of the effects involved, and, subsequently, better agreement with experiment. We also note that the amplitudes of non-linear polarizabilities show relatively weak dependence on the nature of the hybrid functional compared to extreme cases of TD-HF and TD-ALDA. Although pure local and semi-local TD-DFT (without asymptotic correction) is known to err in the description of the charge-transfer states and excitations in extended molecular systems [35], hybrid TD-DFT used in our NLO studies [26,27] offers vast improvements. In addition, optically active one- and two-photon excited states in conjugated molecules do not possess substantial charge-transfer character. In [26,27] we found no indication of incorrect asymptotic behavior of the hybrid functional for conjugated molecules up to 33 Å in length.

Convergence of the third-order response in both molecules with the number of excited states is fast and only a few states are need for most hybrid DFT functionals. For example, 11 excited states is enough to reach the asymptotic limit for functionals with $c_x \leqslant 0.25$. In general, less states are needed for calculations of resonant responses than that in the off-resonant cases. Not all coupling terms in Eq. (2.1) have equal importance. Out of eight terms, typically two terms involving dipole couplings (I and VII terms) provide dominant contributions into the total response. Contributions from the terms, which include Coulomb couplings, grow with increase of an amount of the HF-exchange present in the functional. These results allow one to formulate truncated approaches to calculate NLO responses of large and complex molecular systems at different levels of accuracy.

Acknowledgements

References

[1] H. Kishida, H. Matsuzaki, H. Okamoto, T. Manabe, M. Yamashita, Y. Taguchi, Y. Tokura, Nature 405 (2000) 929.

[2] E.E. Moore, D. Yaron, J. Phys. Chem. A 106 (2002) 5339.

[3] B.H. Cumpston et al., Nature 398 (1999) 51.

[4] Y.Z. Shen, J. Swiatkiewicz, D. Jakubczyk, F.M. Xu, P.N. Prasad, R.A. Vaia, B.A. Reinhardt, Appl. Opt. 40 (2001) 938.

[5] S. Kawata, Y. Kawata, Chem. Rev. 100 (2000) 1777.

[6] N. Dietz, F.L. Madarasz, Mat. Sci. Eng. B 97 (2003) 182.

[7] T. Pons, L. Moreaux, O. Mongin, M. Blanchard-Desce, J. Mertz, J. Biomed. Opt. 8 (2003) 428.

[8] M.G. Silly, L. Porres, O. Mongin, P.A. Chollet, M. Blanchard-Desce, Chem. Phys. Lett. 379 (2003) 74.

[9] C.W. Spangler, J. Mat. Chem. 9 (1999) 2013.

[10] C. Bauer, B. Schnabel, E.B. Kley, U. Scherf, H. Giessen, R.F. Mahrt, Adv. Mat. 14 (2002) 673.

[11] K. Konig, J. Microsc.-Oxford 200 (2000) 83.

[12] W.R. Zipfel, R.M. Williams, R. Christie, A.Y. Nikitin, B.T. Hyman, W.W. Webb, Proc. Natl. Acad. Sci. USA 100 (2003) 7075.

[13] D.R. Kanis, M.A. Ratner, T.J. Marks, Chem. Rev. 94 (1994) 195.

[14] J.L. Brédas, C. Adant, P. Tackx, A. Persoons, B.M. Pierce, Chem. Rev. 94 (1994) 243.

[15] D.B. Cook, Handbook of Computational Quantum Chemistry, Oxford University Press, New York, 1998.

[16] M. Albota et al., Science 281 (1998) 1653.

[17] M. Rumi et al., J. Am. Chem. Soc. 122 (2000) 9500.

[18] J.R. Heflin, K.Y. Wong, O. Zamanikhamiri, A.F. Garito, Phys. Rev. B 38 (1988) 1573.

[19] E. Runge, E.K.U. Gross, Phys. Rev. Lett. 52 (1984) 997.

[20] M.E. Casida, in: D.A. Chong (Ed.), Recent Advances in Density-Functional Methods, Part I, vol. 3, World Scientific, Singapore, 1995.

[21] M.E. Casida, C. Jamorski, K.C. Casida, D.R. Salahub, J. Chem. Phys. 108 (1998) 4439.

[22] F. Furche, R. Ahlrichs, J. Chem. Phys. 117 (2002) 7433.

[23] P. Salek, O. Vahtras, J.D. Guo, Y. Luo, T. Helgaker, H. Agren, Chem. Phys. Lett. 374 (2003) 446.

[24] O. Berman, S. Mukamel, Phys. Rev. A 67 (2003) 42503.

[25] S. Tretiak, V. Chernyak, J. Chem. Phys. 119 (2003) 8809.

[26] A.M. Masunov, S. Tretiak, J. Phys. Chem. B 108 (2004) 899.

[27] G.P. Bartholomew, M. Rumi, S.J.K. Pond, J.W. Perry, S. Tretiak, G.C. Bazan, J. Am. Chem. Soc. (2004) (ASAP).

[28] V. Alain, S. Redoglia, M. Blanchard-Desce, S. Lebus, K. Lukaszuk, R. Wortmann, U. Gubler, C. Bosshard, P. Gunter, Chem. Phys. 245 (1999) 51.

[29] B.J. Orr, J.F. Ward, Mol. Phys. 20 (1971) 513.

[30] S. Tretiak, S. Mukamel, Chem. Rev. 102 (2002) 3171.

[31] A.D. Becke, J. Chem. Phys. 98 (1993) 5648.

[32] M.J. Frisch et al., GAUSSIAN 98 (Revision A.11), Gaussian, Inc., Pittsburgh, PA, 2002.

[33] M. Cossi, V. Barone, J. Chem. Phys. 115 (2001) 4708.

[34] E. Zojer, D. Beljonne, T. Kogej, H. Vogel, S.R. Marder, J.W. Perry, J.L. Bredas, J. Chem. Phys. 116 (2002) 3646.

[35] D.J. Tozer, J. Chem. Phys. 119 (2003) 12697.